PHYSICAL REVIEW B **89**, 041107(R) (2014)

Valley-degenerate two-dimensional electrons in the lowest Landau level

Tomasz M. Kott,* Binhui Hu, S. H. Brown, and B. E. Kane
Laboratory for Physical Sciences and Joint Quantum Institute, University of Maryland, College Park, Maryland 20740, USA
(Received 12 October 2012; revised manuscript received 13 November 2013; published 17 January 2014)

We report low temperature magnetotransport measurements on a high mobility ($\mu = 325\,000$ cm^2/V s) two-dimensional electron system on a H-terminated Si(111) surface. We observe the integral quantum Hall effect at all filling factors $\nu \leqslant 6$ and find that $\nu = 2$ develops in an unusually narrow temperature range. An extended, exclusively even numerator, fractional quantum Hall hierarchy occurs surrounding $\nu = 3/2$, consistent with twofold valley-degenerate composite fermions (CFs). We determine activation energies and estimate the CF mass.

DOI: 10.1103/PhysRevB.89.041107 PACS number(s): 73.40.−c, 71.70.Di, 73.43.−f

Multicomponent two-dimensional (2D) systems in a single Landau level have generated interest due to the possibilities for novel correlated ground states in the integer and fractional quantum Hall (FQH) regimes when the energies of the component states become degenerate. Early experiments focused on measurements of engineered GaAs materials where the spin splitting could be reduced to zero [1–3]. Subsequent development of AlAs quantum wells with a tunable valley degeneracy allowed the study of a spinlike degeneracy in the same limit [4]. Recently, there has been great interest in the sublattice (valley) degeneracy in graphene; experiments show that the valley symmetry affects the FQH hierarchy [5,6] and that valley ferromagnetism occurs when one of two degenerate valleys is occupied [7].

Measurements on silicon, the first multivalley system to be considered theoretically [8,9], had been hampered by high disorder. Lately, however, Si(100)/SiGe heterostructures have shown mobilities up to 10^6 cm^2/V s [10]. Nonetheless, Si(100) is known to have an intrinsic valley splitting due to the confinement potential [11–14]. The case of 2D electrons on (111) oriented silicon surfaces, which have three pairs of opposite momentum ($\vec{k}$) valleys, is especially interesting [15]. As opposed to either AlAs or Si(100), the degeneracy of valley pairs with $\pm\vec{k}$ symmetry in Si(111) cannot be broken within the effective mass approximation or by a confinement potential [9], similar to the case of valleys in graphene. Additionally, both AlAs and Si(111) exhibit anisotropic mass tensors; in AlAs, this anisotropy arguably transfers to composite fermions (CFs) [16]. Novel broken symmetry states have been predicted at integer filling factor ν, when the Fermi energy E_F lies between two valleys with different mass tensors [17].

In this Rapid Communication we present transport data on a very high mobility electron system ($\mu = 325\,000$ cm^2/V s at a temperature $T = 90$ mK and density $n_s = 4.15 \times 10^{11}$ cm^{-2}) on a hydrogen-terminated Si(111) surface. We observe an extended FQH hierarchy around $\nu = 3/2$. We argue that the FQH hierarchy is consistent with the SU(2) symmetry of a twofold valley-degenerate ground state and present the first measurement of the CF mass in a multicomponent system, as well as the first in an anisotropic system. We also present preliminary evidence for many-body interactions affecting integer activation energies: The development of $\nu = 2$ occurs in an unusually narrow temperature range, which may signal a transition to broken symmetry valley states.

For our samples, we replace the Si-SiO_2 interface of a typical metal-oxide-semiconductor field-effect transistor with an interface between H-terminated Si(111) and a vacuum dielectric in order to remove the effects of strain and dangling bonds from the Si(111) surface [18]. An encapsulating silicon-on-insulator piece is bonded via van der Waals forces to the high resistivity H-Si(111) substrate ($< 0.5^\circ$ miscut) and forms a gate. The sample studied in the present work is fabricated in the same way as previous ones, with further optimized cleaning and annealing steps [19]. Four-terminal resistance in a square van der Pauw geometry is defined as $R_{ij,lm} = V_{lm}/I_{ij}$, with $R_{xx} = R_{12,34}$ and $R_{yy} = R_{24,13}$ oriented along the $[1\bar{1}0]$ and $[11\bar{2}]$ directions, respectively [see inset to Fig. 1(a)]. Hall traces ρ_{xy} are the averages of $R_{14,23}$ and $R_{23,14}$ to prevent mixing. The data were obtained at densities between $n_s = 3.7$ and 5.7×10^{11} cm^{-2}, adjustable via a gate voltage, in both a ^{3}He system and ^{3}He/^{4}He dilution system with base temperatures of 280 and 90 mK, respectively. The density range is limited at high n_s due to gate leakage and at low n_s due to nonlinear contact resistances and a small parallel conductance channel, which are responsible for nonzero minima at some integer filling factors. Magnetotransport measurements were performed using standard lock-in techniques with a typical excitation of 1–25 nA at 5 Hz in a magnetic field B up to 12 T.

Figure 1(a) shows R_{xx}, R_{yy}, and ρ_{xy} versus B taken at $T = 90$ mK and density $n_s = 3.75 \times 10^{11}$ cm^{-2}. Shubnikov–de Haas oscillations (SdHO) are visible down to about $B \sim 0.15$ T. The differences in the position of the minima at low B between R_{xx} and R_{yy} are not an indication of density inhomogeneity; high B minima of R_{xx} and R_{yy} are consistent to 0.01% at $\nu = 8/5$. While $R_{xx} \approx R_{yy}$ at $B = 0$, strong anisotropy appears for $B > 0$. Such anisotropy is to be expected in Si(111) when valleys with different mass tensors have an unequal density of states at E_F. Here, we simply note that the anisotropy is essentially constant above $B = 7$ T, and we will focus our analysis on these higher magnetic fields. By $B \approx 1.3$ T ($\nu = 12$), only the lowest Landau level is occupied. As B increases, the sixfold valley degeneracy breaks. Below $\nu = 8$ all integer filling factors have minima, with the even states ($\nu = 6$, 4, and 2) being stronger than the odd ($\nu = 3$, 5, and 7).

Figure 1(b) shows the temperature dependence of R_{xx} and R_{yy} in the FQH regime below $\nu = 2$. In this range, we observe minima at nine fractions: $\nu = 8/5, 14/9, 20/13, 22/15, 16/11, 10/7, 4/3$, (shown) as well as 6/5 and 14/11 at lower densities

*Present address: Johns Hopkins University Applied Physics Laboratory, Laurel, MD 20723, USA; tkott@mailaps.org

 ©2014 American Physical Society

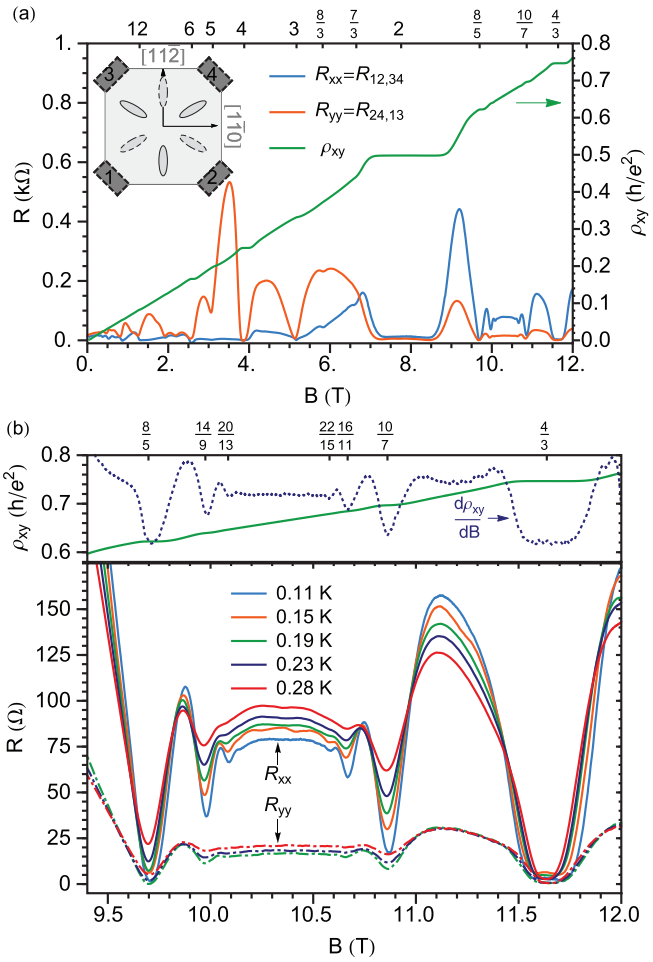

FIG. 1. (Color) (a) R_{xx}, R_{yy} (left), and ρ_{xy} (right) vs B at $T = 90$ mK and $n_s = 3.75 \times 10^{11}$ cm^{-2} with filling factors listed on the top axis; the fractional states at $\nu = \frac{8}{5}$, $\frac{10}{7}$, and $\frac{4}{3}$ have plateaus in ρ_{xy}. (b) R_{xx} and R_{yy} vs B for $n_s = 3.75 \times 10^{11}$ cm^{-2}. Seven FQH states are visible at $T = 110$ mK; the filling factors are labeled on the top axis. Top panel: ρ_{xy} vs B for $T = 110$ mK. The derivative is also shown to accentuate the fine structure, matching the R_{xx} minima.

(not shown). Hall plateaus at $\nu = 8/5$ and $4/3$ are quantized to within 0.5% of their nominal values. For weaker fractions, ν is determined from B evaluated at the resistance minimum relative to the value of B at the sharp minimum of $8/5$. Using this technique all fractions deviate less than 0.1% from their designated values.

The hierarchy of observed states is exactly that predicted by an SU(2) symmetry in which the twofold valley degeneracy of electrons is preserved, leading to the creation of CFs with two and four attached vortices (^{2}CF and ^{4}CF, respectively) [20]. For the hierarchy of fractional states around $\nu = 3/2$, which are the hole-symmetric equivalents to the $\nu = 1/2$ states, the filling factor ν^* of CFs is given by $\nu = 2 - \nu^*/(2p\nu^* \pm 1)$ [20], where $p = 1$ and 2 for ^{2}CF and ^{4}CF, respectively. With an SU(2) symmetry, only $\nu^* = 2,4,6,\ldots$ are expected, giving rise to the hierarchy visible in Fig. 1(b). A similar, though smaller, hierarchy was observed recently in graphene with the same conclusion [6]. Finally, $\nu = 6/5$ and $14/11$ relate to ^{4}CFs via $\nu^* = 4/3$ and $8/5$, respectively, using $2 - \nu^*/(2\nu^* - 1)$; the ^{4}CF hierarchy simply reflects the FQH states of ^{2}CFs. We note that we observe no evidence for a $\nu = 5/3$ state, similar to recent experiments in both graphene [6] and Si/SiGe [10]. However, the 5/3 state is visible in nominally doubly degenerate AlAs, probably due to local strains [17,21,22].

To estimate the mass of the CFs, we use the theory of SdHO and apply it to $\nu = 3/2$ by transforming to an effective magnetic field $B_{\rm eff} = 3(B - B_{3/2})$ where $B_{3/2} = 10.34$ T (calculated from the density) [23]. Although we could use either activation energy measurements or SdHO to find the gaps, analysis based on SdHO takes into account intrinsic level broadening. We first compute the amplitude ΔR of the oscillations using a linear interpolation of the minima and maxima (see Ref. [24]). We then use $\Delta R \propto R_0 \exp\{-\pi\Gamma/\Delta\}\xi/\sinh\xi$, where $\xi = 2\pi^2 T/\Delta$ and R_0 is the (temperature dependent) resistance at $B_{\rm eff} = 0$, to find the gap Δ (Γ quantifies the intrinsic level broadening of Landau levels).

The extracted SdH data is shown in Fig. 2(a); the vertical bars show the measurement errors in resistance minima. Note that due to temperature constraints, there are only three data points available for R_{yy} data—this means that a straightforward comparison of masses extracted from R_{yy} and R_{xx} data will not have the same precision. Additionally, it is important to note that while we extract two masses ($m_{xx}^{\rm CF}$ and $m_{yy}^{\rm CF}$), we do not claim that these are aligned to the principal axes of the effective mass tensor (due to the van der Pauw geometry). Therefore, we cannot make any statement about the possible anisotropy of composite fermion masses as is argued by Gokmen *et al.* [16].

We expressly assume that $\Delta_{\rm CF} = \hbar\omega_c^{\rm CF}$, $\omega_c^{\rm CF} = e|B_{\rm eff}|/m_{\rm CF}$ and extract $m_{xx,yy}^{\rm CF}$ directly. The results are shown in Fig. 2(b). There are two distinct errors that are not shown. First is the statistical error due to the fitting process. For all cases but one, this is less than 10%, and for all $m_{xx}^{\rm CF}$ values it is less than 3%. The second error is the error due to lack of data. While harder to quantify, it is clear that the $m_{xx}^{\rm CF}$ values, based on five temperature values, are more robust than the $m_{yy}^{\rm CF}$ values.

By considering the extracted SdH gap energies, however, we note that the values for both directions are consistent with activation energy data; in Fig. 2(c), we plot the gap energy $\Delta_{\rm CF}$ as a function of $B_{\rm eff}$. The activation energy at $\nu = 4/3$, measured from higher T data, is consistent with a constant value for $m_{\rm CF}$. Additionally, we find that all of the FQH data for R_{xx} collapse onto a single line for $\Delta R \sinh\xi/R_0\xi$ vs $1/B$ with $\Gamma^{\rm CF} = 0.83 \pm 0.04$ K, somewhat less than twice as large as the value for electrons, $\Gamma = 0.49 \pm 0.02$ K, determined at low B using the same approach.

For comparison to other systems, we define a normalized CF mass $m_{\rm nor}^{\pm} = m_{\rm CF}\epsilon/\sqrt{B}$ (in units of $m_e\,T^{-1/2}$, where the $\pm$ is the sign of $B_{\rm eff}$) [25]. Using $\epsilon = 6.25$ $[(\epsilon_{\rm Si} + \epsilon_{\rm Vac})/2$, a value appropriate at a silicon-vacuum interface for an electron gas with a perpendicular extent $z_\perp$ small compared to the interaction distance] a weighted average for R_{xx} data gives $m_{\rm nor}^{-} = 2.14 \pm 0.04$ and $m_{\rm nor}^{+} = 2.40 \pm 0.05$. In other materials, $m_{\rm nor} \approx 3.2$–3.5 for GaAs at $\nu = 1/2$ (Ref. [26], and references therein) or $m_{\rm nor} \approx 1.7$ at $\nu = 3/2$ [23], and $m_{\rm nor} \approx 1.1$–1.3 for ZnO at $\nu = 1/2$ [27]. Unlike our samples, the data

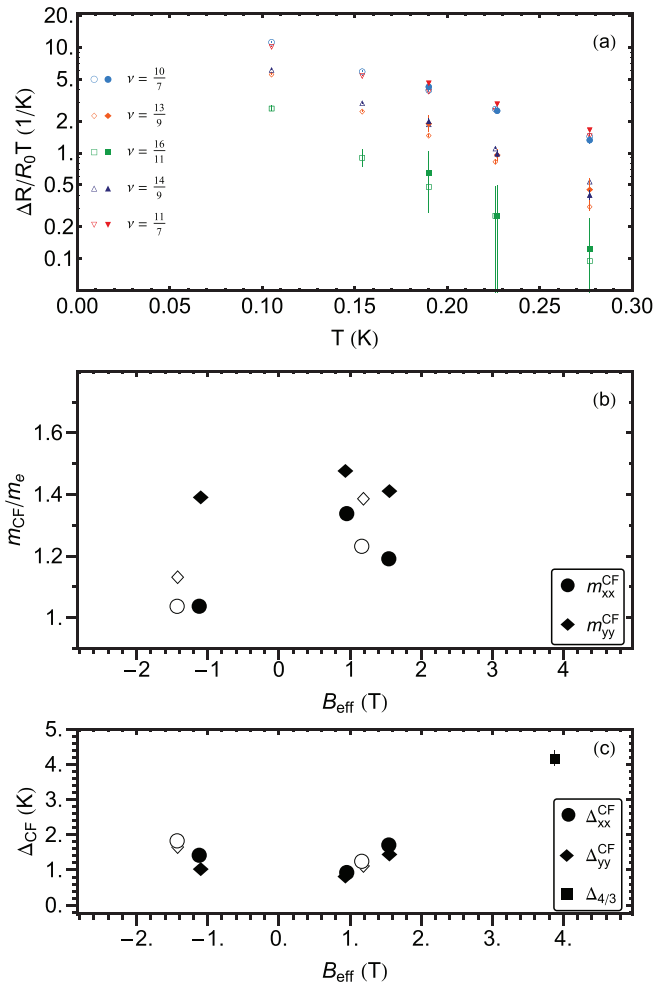

FIG. 2. (Color) (a) Resistance data (with measurement errors) versus temperature used in Shubnikov–de Haas analysis. Open (closed) symbols are from R_{xx} (R_{yy}). Note that only three data points are available for all R_{yy} data. (b) Mass of composite fermions assuming that the gaps probed by Shubnikov–de Haas (SdH) oscillations have the form $\Delta_{\rm CF} = \hbar\omega_c^{\rm CF}$. Open symbols indicate values extracted from maxima. See text for a discussion of the statistical and systematic errors involved in this measurement. (c) Equivalent CF gap energy calculated from the masses. The gap value at $\nu = 4/3$ is calculated from activation energy data and is approximately the same for both R_{xx} and R_{yy}.

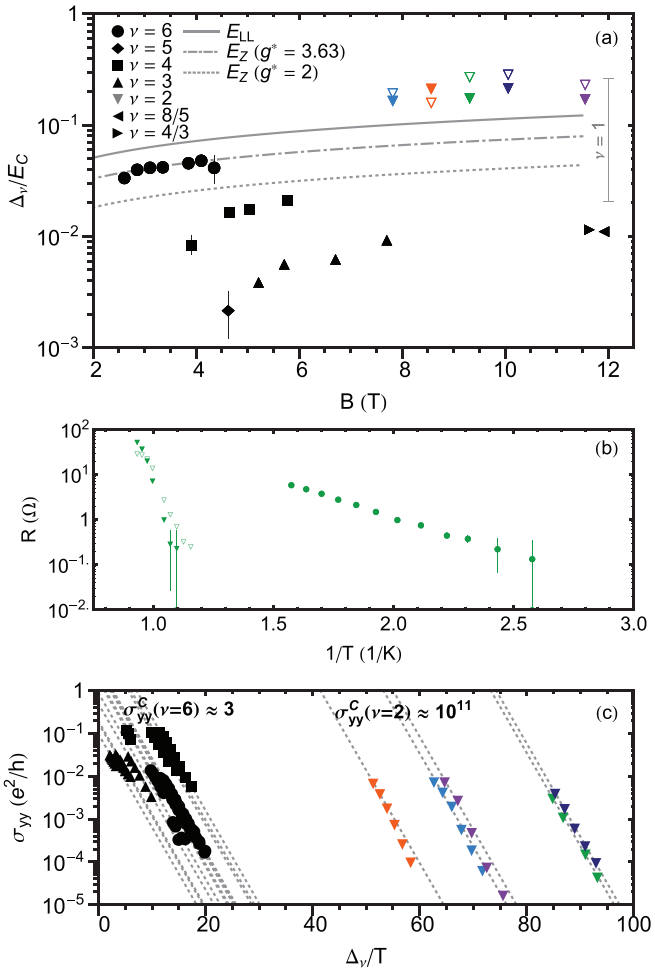

FIG. 3. (Color) (a) Activation energy measurements as a function of B in units of Coulomb energy. Vertical bars show the 95% confidence errors from fits to the linear portions of Arrhenius plots. Closed (open) symbols indicate data from R_{yy} (R_{xx}) measurements. The $\nu = 2$ data shows an enhanced energy gap greater than the Landau level spacing ($E_{\rm LL}$) and indicates the scatter between R_{xx} and R_{yy} data. (b) Arrhenius plot of R for $\nu = 2$ and 6 at $n_s = 4.74 \times 10^{11}$ cm^{-2}. While the $\nu = 6$ dependence is linear over a wide range of temperatures, the $\nu = 2$ data show a very narrow linear region. Both R_{xx} (open symbols) and R_{yy} (closed) show this effect for $\nu = 2$. (c) Plot of the linear portion of σ_{yy} versus Δ_ν/T, showing the difference between the critical conductivities $\sigma_{yy}^C = \sigma_{yy}\,(1/T \to 0)$ at different filling factors and densities.

for GaAs experiments appears to be symmetric around $B_{\rm eff} = 0$ T. Furthermore, the ZnO heterostructures show a linear dependence on the perpendicular magnetic field. Our results cannot rule out either a divergence or a linear dependence on B. There are several material-specific effects that may affect the CF mass, including effective-mass anisotropy [28], the finite $z_\perp$ of the electron gas, and Landau level mixing [29,30]. The modification of short-range interactions due to the large dielectric-constant ϵ mismatch at the surface is particularly relevant for our devices.

We turn now to gaps at integer filling factors; we use the T dependence of R_{xx} and R_{yy} to calculate the activation energies via $R \propto \exp(-\Delta_\nu/2k_BT)$. By changing n_s, we are able to measure the gap Δ_ν as a function of B: Figure 3(a) shows the results of such an analysis in units of the Coulomb energy $E_C = e^2/4\pi\epsilon\epsilon_0 l_B$, where $l_B = \sqrt{\hbar/eB}$ and we use $\epsilon = 6.25$. Due to anisotropy and a lack of large resistance range in R_{xx}, we show only Δ_ν^{yy} for most of the filling factors; for $\nu = 2$ we show both transport directions as an example of scatter in the gap energy.

With the assumption that the valley splitting is smaller than the Zeeman gap, the $\nu = 6$ activation energy is interpreted as $\Delta_6 = E_Z = g^*\mu_B B_{\rm tot}$, from which we estimate $g^* = 3.63 \pm 0.06$, consistent with previous measurements [18,19]. The presence of minima at all filling factors $\nu \leqslant 6$ suggests a B-dependent valley splitting, similar to that observed in SiGe heterostructures [31,32]. Indeed, the appearance of odd $\nu < 6$ shows that high magnetic fields increasingly break the twofold

degeneracy of opposite $\vec{k}$ valleys. The estimate at $\nu = 5$ is based on a "strength" (S) of the state defined as the ratio of the resistance minimum to the average of the adjacent maxima [10]. From the T dependence, we can estimate a quasigap; the state is weaker than any other filling factor $\nu \leqslant 6$. For $\nu = 1$, we can only estimate an upper and lower bound while noting that the minimum remains visible at $T = 1$ K [see Fig. 3(a)]. The odd filling factor gaps, which are much greater than Γ, indicate that the splitting is likely due to many-body effects.

For $\nu = 2$, the interpretation of the activation energy is more difficult. As shown by the solid line in Fig. 3(a), $\Delta_{\nu=2}$ is greater than the Landau level spacing (E_{LL}). To show the qualitative difference between $\nu = 2$ and the much better understood $\nu = 6$, we show the temperature dependence of the resistance for the two minima in Fig. 3(b) at a density of $n_s = 4.60 \times 10^{11}$ cm^{-2}. The data for $\nu = 6$ clearly follow an Arrhenius relationship, while the resistance change for $\nu = 2$ occurs over a very limited temperature change, and has a much smaller range over which it is linear. The transition for $\nu = 2$ occurs in a range of $\sim$200 mK near $T \approx 1$ K. Another illustration of the peculiarity of $\nu = 2$ is shown in Fig. 3(c), where the thermally activated portion of σ_{yy} as a function of Δ_ν/T is plotted for integer filling factors. The critical conductivity $\sigma_{yy}^C = \sigma_{yy}\,(1/T \to 0)$ typically observed in the integral quantum Hall regime is $\sim 2e^2/h$, with reductions possible due to short-range scattering and screening [33–35]. In our data we observe that the criticial conductivity at $\nu = 2$ is 10–16 orders of magnitude larger than σ_{yy}^C at higher filling factors. We therefore consider other interpretations for the large activation energy.

At $\nu = 2$ one pair of valleys is filled, so added electrons must occupy a new valley with a different mass tensor. In this regime, Abanin *et al*. [17] predict a novel nematic phase with the electron gas broken up into domains of differing valley polarization. Indeed, it is characterized by a very narrow T range where R is thermally activated, leading to a large extrapolated R for $1/T \to 0$ in an Arrhenius plot of the data. Abanin *et al*. argue that in an anisotropic valley-degenerate system, the transport mechanism in the limit of valley-polarized domains is variable-range hopping due to the low T localization of edge currents along domain walls separating areas of different valley polarization. Fits of the temperature-dependent resistance to different models, including $\sigma = (\sigma^{C*}/T)\exp\{\Delta_\nu/2k_BT\}$, reproduce the large energy gap and do not reduce the discrepancy in σ_{yy}^C [35].

In summary, we have shown evidence of electron-electron interactions in a high mobility Si(111) system. The sixfold valley degeneracy breaks at high magnetic fields into an apparent SU(2) symmetry reflected by the fractional quantum Hall state hierarchy. While the SU(2) symmetry is not unexpected due to the underlying valley structure of Si(111), the extended hierarchy reiterates the need to fully understand the valley degeneracy breaking mechanism in this system. We estimated the mass of composite fermions near $\nu = 3/2$ by assuming that the Shubnikov–de Haas oscillation gaps can be interpreted as a cyclotron energy. Further experiments are necessary. First, hexagonal samples would allow unambiguous measurements of ρ on Si(111) surfaces. Second, higher magnetic fields are necessary to probe the $\nu < 1$ regime at similar densities, which would shed further light on the valley degeneracy of composite fermions. Finally, tilted magnetic fields would introduce controlled valley splitting of inequivalent valleys [18,36] and in particular would help shed light on the behavior at $\nu = 2$.

This work was funded by the Laboratory for Physical Sciences. The authors thank Jainendra Jain for useful discussions.

[1] D. R. Leadley, R. J. Nicholas, D. K. Maude, A. N. Utjuzh, J. C. Portal, J. J. Harris, and C. T. Foxon, Phys. Rev. Lett. **79**, 4246 (1997).

[2] W. Kang, J. B. Young, S. T. Hannahs, E. Palm, K. L. Campman, and A. C. Gossard, Phys. Rev. B **56**, R12776 (1997).

[3] S. P. Shukla, M. Shayegan, S. R. Parihar, S. A. Lyon, N. R. Cooper, and A. A. Kiselev, Phys. Rev. B **61**, 4469 (2000).

[4] M. Shayegan, E. P. De Poortere, O. Gunawan, Y. P. Shkolnikov, E. Tutuc, and K. Vakili, Phys. Status Solidi B **243**, 3629 (2006).

[5] C. R. Dean, A. F. Young, P. Cadden-Zimansky, L. Wang, H. Ren, K. Watanabe, T. Taniguchi, P. Kim, J. Hone, and K. L. Shepard, Nat. Phys. **7**, 693 (2011).

[6] B. E. Feldman, B. Krauss, J. H. Smet, and A. Yacoby, Science **337**, 1196 (2012).

[7] A. F. Young, C. R. Dean, L. Wang, H. Ren, P. Cadden-Zimansky, K. Watanabe, T. Taniguchi, J. Hone, K. L. Shepard, and P. Kim, Nat. Phys. **8**, 550 (2012).

[8] M. Rasolt, F. Perrot, and A. H. MacDonald, Phys. Rev. Lett. **55**, 433 (1985).

[9] M. Rasolt, B. I. Halperin, and D. Vanderbilt, Phys. Rev. Lett. **57**, 126 (1986).

[10] T. M. Lu, W. Pan, D. C. Tsui, C.-H. Lee, and C. W. Liu, Phys. Rev. B **85**, 121307 (2012).

[11] T. B. Boykin, G. Klimeck, M. A. Eriksson, M. Friesen, S. N. Coppersmith, P. von Allmen, F. Oyafuso, and S. Lee, Appl. Phys. Lett. **84**, 115 (2004).

[12] D. C. Tsui and G. Kaminsky, Phys. Rev. Lett. **42**, 595 (1979).

[13] K. Takashina, Y. Ono, A. Fujiwara, Y. Takahashi, and Y. Hirayama, Phys. Rev. Lett. **96**, 236801 (2006).

[14] S. Goswami, K. A. Slinker, M. Friesen, L. M. McGuire, J. L. Truitt, C. Tahan, L. J. Klein, J. O. Chu, P. M. Mooney, D. W. van der Weide, R. Joynt, S. N. Coppersmith, and M. A. Eriksson, Nat. Phys. **3**, 41 (2007).

[15] E. H. Hwang and S. Das Sarma, Phys. Rev. B **87**, 075306 (2013).

[16] T. Gokmen, M. Padmanabhan, and M. Shayegan, Nat. Phys. **6**, 621 (2010).

[17] D. A. Abanin, S. A. Parameswaran, S. A. Kivelson, and S. L. Sondhi, Phys. Rev. B **82**, 035428 (2010).

[18] K. Eng, R. N. McFarland, and B. E. Kane, Phys. Rev. Lett. **99**, 016801 (2007).

[19] R. N. McFarland, T. M. Kott, L. Sun, K. Eng, and B. E. Kane, Phys. Rev. B **80**, 161310 (2009).

[20] K. Park and J. Jain, Solid State Commun. **119**, 291 (2001).
[21] M. Padmanabhan, T. Gokmen, and M. Shayegan, Phys. Rev. Lett. **104**, 016805 (2010).
[22] Y. P. Shkolnikov, S. Misra, N. C. Bishop, E. P. De Poortere, and M. Shayegan, Phys. Rev. Lett. **95**, 066809 (2005).
[23] R. Du, A. Yeh, H. Stormer, D. Tsui, L. Pfeiffer, and K. West, Surf. Sci. **361-362**, 26 (1996).
[24] M. Padmanabhan, T. Gokmen, N. C. Bishop, and M. Shayegan, Phys. Rev. Lett. **101**, 026402 (2008).
[25] B. I. Halperin, P. A. Lee, and N. Read, Phys. Rev. B **47**, 7312 (1993).
[26] W. Pan, H. L. Stormer, D. C. Tsui, L. N. Pfeiffer, K. W. Baldwin, and K. W. West, Phys. Rev. B **61**, R5101 (2000).
[27] D. Maryenko, J. Falson, Y. Kozuka, A. Tsukazaki, M. Onoda, H. Aoki, and M. Kawasaki, Phys. Rev. Lett. **108**, 186803 (2012).
[28] B. Yang, Z. Papic, E. H. Rezayi, R. N. Bhatt, and F. D. M. Haldane, Phys. Rev. B **85**, 165318 (2012).
[29] P. J. Gee, F. M. Peeters, J. Singleton, S. Uji, H. Aoki, C. T. B. Foxon, and J. J. Harris, Phys. Rev. B **54**, R14313 (1996).
[30] V. Melik-Alaverdian and N. E. Bonesteel, Phys. Rev. B **52**, R17032 (1995).
[31] P. Weitz, R. Haug, K. von. Klitzing, and F. Schäffler, Surf. Sci. **361-362**, 542 (1996).
[32] M. A. Wilde, M. Rhode, C. Heyn, D. Heitmann, D. Grundler, U. Zeitler, F. Schäffler, and R. J. Haug, Phys. Rev. B **72**, 165429 (2005).
[33] N. d'Ambrumenil, B. I. Halperin, and R. H. Morf, Phys. Rev. Lett. **106**, 126804 (2011).
[34] D. G. Polyakov and B. I. Shklovskii, Phys. Rev. Lett. **74**, 150 (1995).
[35] Y. Katayama, D. C. Tsui, and M. Shayegan, Phys. Rev. B **49**, 7400 (1994).
[36] T. Gokmen, M. Padmanabhan, O. Gunawan, Y. P. Shkolnikov, K. Vakili, E. P. De Poortere, and M. Shayegan, Phys. Rev. B **78**, 233306 (2008).